Bioinspired Enzymatic Mineralization Incorporates $CaCO_3$ Mesocrystals in Wood for Surface Reinforcement and Flame-Retardancy

Tian Fei[1], Han-Jing Yi[1], Robert Zboray[2], Xiao-Qiang Yan[1], Si-Si Song[1], Lei Ren[1], Huizhang Guo[3], Yuan Jiang[1,4*]*

[1] College of Materials, State Key Laboratory of Marine Environmental Science, Fujian Key Laboratory of Advanced Materials, Higher Educational Key Laboratory for Biomedical Engineering of Fujian Province, Xiamen University, Xiamen 361005, P.R. China

[2] Centre for X-ray Analytics, Empa Dübendorf, 8600 Dübendorf, Switzerland

[3] Wood Materials Science, ETH Zürich, 8093 Zürich, Switzerland

[4] State Key Laboratory of Silicon Materials, Zhejiang University, Hangzhou 310027, P.R. China

Emails: renlei@xmu.edu.cn, yuan.jiang@xmu.edu.cn

This document is the accepted manuscript version of the following article:
Fei, T., Yi, H. J., Zboray, R., Yan, X. Q., Song, S. S., Ren, L., … Jiang, Y. (2022). Bioinspired enzymatic mineralization incorporates CaCO3 mesocrystals in wood for surface reinforcement and flame-retardancy. ACS Sustainable Chemistry and Engineering, 10(49), 16118-16124. https://doi.org/10.1021/acssuschemeng.2c05094

ABSTRACT: The development of sustainable strategies for the integration of wood with excellent mechanical and fire-retardant properties is increasingly appealing to bridge this renewable engineering material with multiple emerging applications. Inspired by biomineralization on soft tissues for a protective function, we developed enzymatic mineralization for the deposition of $CaCO_3$ minerals in wood compartments. The immobilized urease in vessels and fibers increased the local concentration of bicarbonate anions, which, together with the directional diffusion of calcium cations, caused the deposition of calcitic $CaCO_3$ mineral preferentially in cellular compartments of cells near the wood surface. The employment of the polymeric additives ensured that multistage mineralization started on the lumen-facing cell wall surfaces, and the local space in the lumina was filled with mesocrystalline $CaCO_3$ deposits after multiple rounds of enzymatic mineralization. The incorporation of rod-shaped $CaCO_3$ mesocrystals resulted in mineralized wood with improved surface hardness, and flame retardancy, while at the same time, the moderate incorporation level preserved the intrinsic lightweight merit of wood. This bioinspired enzymatic mineralization approach can regulate the positioning and structure of functional minerals for the fabrication of high-performance mineralized wood in a sustainable manner.

KEYWORDS: wood, bioinspiration, enzymatic mineralization, calcium carbonate, reinforcement, flame retardancy

INTRODUCTION

Present industrial development requires strong and tough lightweight engineering materials for construction, transportation, packing, and energy storage and conversion produced in a sustainable manner[1, 2]. Wood has an ecological advantage compared to synthetic materials like plastic, concrete, and steel, because the former is a renewable natural resource with a negative carbon footprint[3-8]. Wood is composed of elongated cells, most of which are oriented in the longitudinal direction with a hollow lumen at the microscale and are connected via pits or perforations[9, 10]. At the ultrastructural level of wood, the cell walls consist mainly of cellulose, hemicellulose, and lignin[11-13]. Cellulose microfibrils aggregates with a width of ~20 nm form a skeleton, which is surrounded by hemicelluloses and lignin functioning as a matrix. As a result, wood exhibits high stiffness and strength relative to its low apparent density.[9]

Fabrication of wood composites[5, 14] may enable the utilization of fast-growing timbers as structural materials in urban areas[15, 16], because fast growing timbers typically face the challenge of poor mechanical properties[7, 17-19] and low flame retardancy[19-24]. Consequently, modifications are necessary for engineering applications[25-28]. Mineralization, which integrates a stiff inorganic phase in the organic wood scaffold can be a wood modification strategy. However, current treatments either result in a severe mass gain of the composite[23, 26] or demolish its cellular structure[7, 29], which sacrifice the intrinsic lightweight merit of wood. Therefore, emerging methods are required to deliver wood with a minimum of density increase, but with a significant enhancement in mechanical performance and flame retardancy via a sustainable approach[17]. To this end, bioinspired mineralization can become a practical approach to achieving multifunctional composite wood and contribute to the design principles of stiffening soft materials with mineral structures[4, 13, 30]. It is nonetheless challenging to modify the complex hierarchical wood structure

by bioinspired mineralization. The primary challenge is the rather unknown correlation between the shape information of the embedded minerals and the functional performance[31]. Design of controllable routes to achieving the related forms is another challenge, as the hierarchical porous framework strongly increases the diffusion distance of reacting chemicals and therefore, the maintenance of high supersaturation levels in the cell lumina is increasingly difficult in the course of mineralization. Third, the presence of embedded minerals in cell lumina can lead to an increase of stiffness and strength in composite wood, but at the same time it may inevitably sacrifice density and toughness[19, 23]. Hence, it is worth noting that besides the introduction of emerging functions, the evaluation of mass gain by mineralization is equivalently important, as in comparison with conventional engineering materials, wood is advantageous for a low density in view of its functionalities[6, 17].

The anisotropic microstructure of wood can direct the orientation and distribution of mineral particles, as known for petrified wood[32]. Although bioinspired strategies show great potential for design of advanced engineering materials[4, 30, 33], they have been rarely implemented to date, especially, in terms of upscaling and cost. In this work, we report on enzymatic mineralization, which can lead to the *in-situ* deposition of mesocrystalline $CaCO_3$ microrods in lumina of cells near the wood surface, and therefore, generate a mineralized wood with impact on surface hardening and flame-retardancy. The scheme of enzymatic mineralization is shown in Figure 1a. Urease was immobilized in cell lumina to ensure mineralization occurs preferentially in the wood structure (Figure 1). Multiple rounds of enzymatic mineralization were carried out to ensure sufficient deposition. Micro-computed tomography (microCT), scanning electron microscopy (SEM), and Raman microscopy were used to study the spatial distribution of the deposits and the related structural features. Wood samples treated for various periods of mineralization were

characterized with SEM to reveal the related growth mechanisms. Surface hardness tests were conducted for the evaluation of the mechanical properties of native and mineralized wood. The limiting oxygen index (LOI) test allowed to define a fire-retardant level of the wood before and after enzymatic mineralization.

RESULTS AND DISCUSSION

An enzymatic mineralization was developed to deposit $CaCO_3$ in poplar wood (Figure 1a). In a standard mineralization protocol, a wood block ($30 \times 2 \times 2$ mm^3 (L × T × R)) loaded with urease beforehand was infiltrated with the precursor solution containing calcium cations (20 mM), urea (25 mM), and poly(aspartic acid) (PAsp; 0.01 g L^{-1}). Urease anchored to the cellular wall surfaces (Figure s1) beforehand catalyzed the hydrolysis of urea to produce bicarbonate anions, which increased the local concentrations of the reacting anions as well as the pH value. The calcium cations in the bulk phase diffused continuously into wood cell lumina to interact with bicarbonate anions, which led to the deposition of $CaCO_3$ minerals. PAsp was indispensable for the preferential deposition of $CaCO_3$ mineral in wood cells lumina, and in the meantime, the reacting mother liquor remained clear in the course of enzymatic mineralization. As a comparison, its absence led to the unselective precipitation of $CaCO_3$ minerals both in wood and in bulk phase. Previous studies of bioinspired mineralization reported that the soluble polymeric additives such as PAsp could promote the heterogeneous nucleation of $CaCO_3$[34-36]. Up to three circles of mineralization were run to achieve deposition of $CaCO_3$ in wood cell lumina.

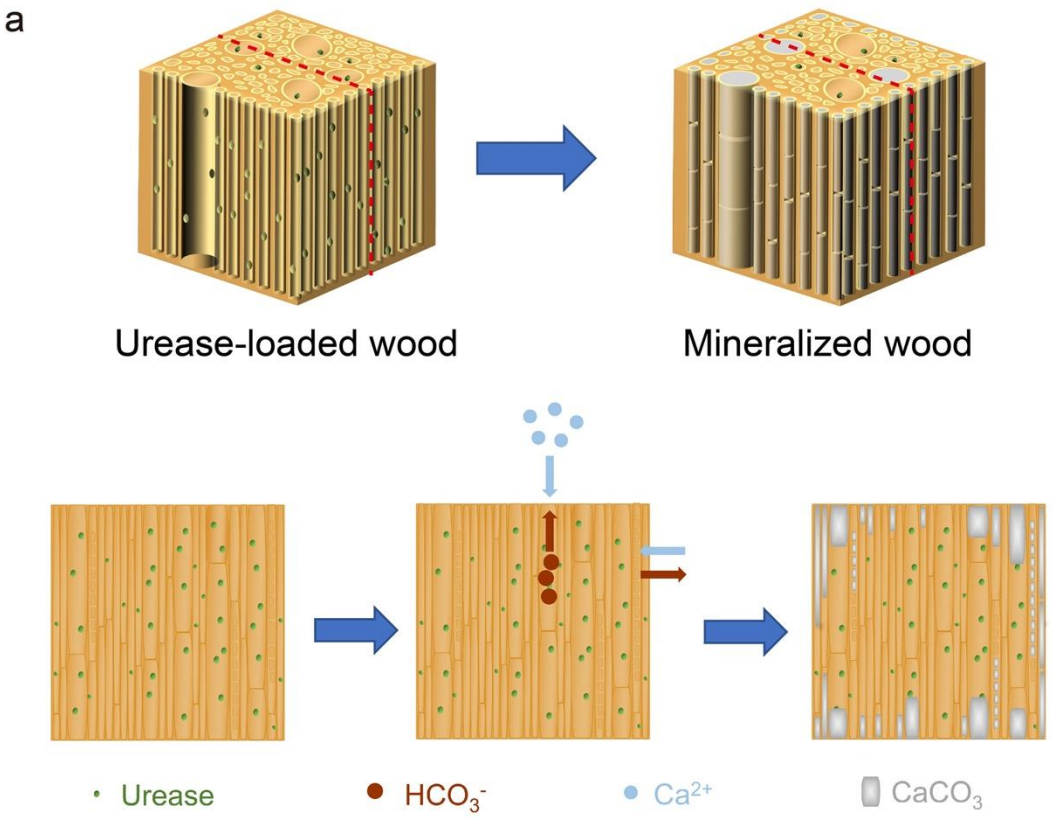
a
Urease-loaded wood
Mineralized wood
Urease
HCO_3^-
Ca^{2+}
$CaCO_3$

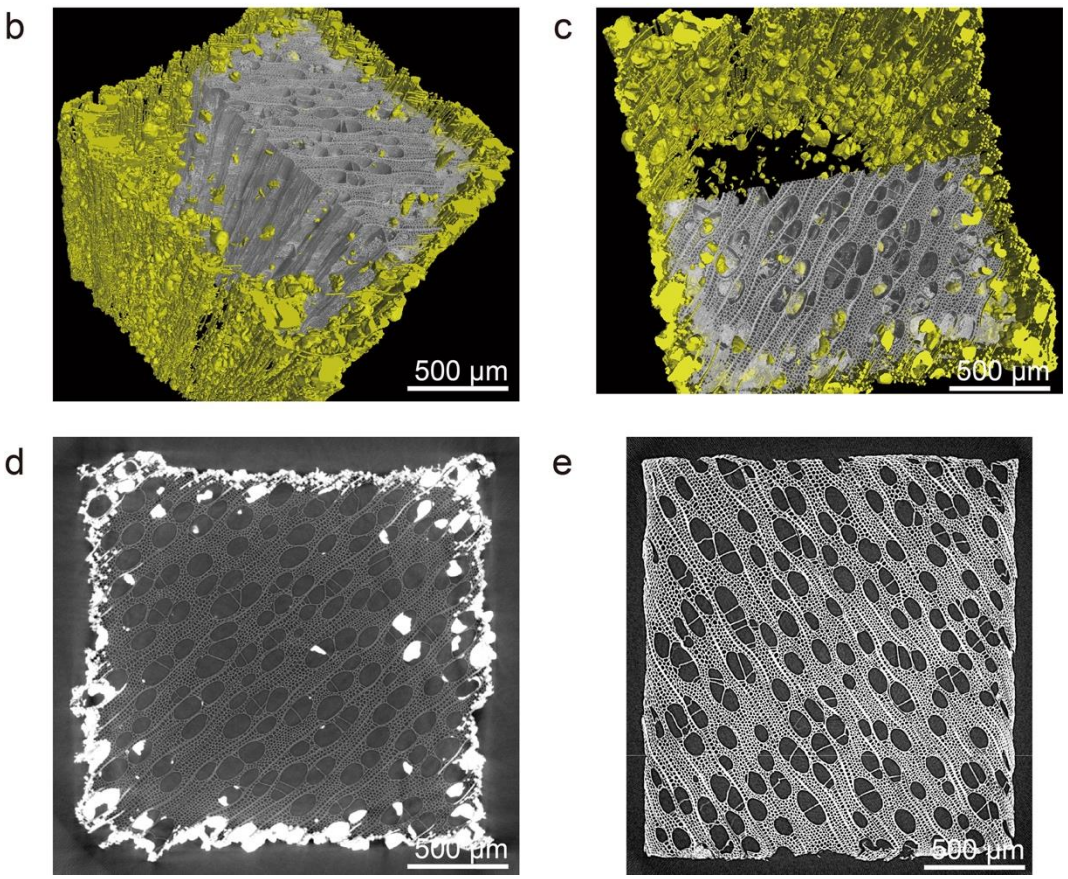
b
500 μm
c
500 μm
d
500 μm
e
500 μm

Figure 1. (a) Schematic of the enzymatic mineralization process which leads to the *in-situ* deposition of $CaCO_3$ mineral in wood cell lumina. (b-e) Micro computed X-ray tomography images of the mineralized wood (b-d) and native wood (e), where 3D reconstruction displays the spatial distribution of the $CaCO_3$ constituents in wood cell lumina. In images b-c, the yellow and gray colors represent the $CaCO_3$ and wood constituents, respectively. In images d-e, the white and gray colors represent the $CaCO_3$ and wood constituents, respectively.

Micro computed X-ray tomography (microCT) was used to identify the spatial distribution of the $CaCO_3$ constituents in poplar wood (Figure 1b-d). Compared with the honeycomb cells of native wood (Figure 1e), the occurrence of mineral particles was revealed in wood cell lumina including vessels and fibers, the vast majority of which were positioned in the marginal area of the wood surface. The preferential positioning can be ascribed to the establishment of local supersaturation levels in wood. The decomposition of urea caused by the presence of urease in wood cells led to the spontaneous permeation of bicarbonate anions out of the wood block, while the directional diffusion of calcium cations was in the contrary direction. Hence, a high supersaturation level may have been established in the marginal area of the wood block, where the deposition of $CaCO_3$ minerals occurred eventually.

A micro computed X-ray tomographic image confirms that the mineral particles incorporated in wood cells are rod in shape (Figure 2a). To facilitate the structural analyses, the mineral particles were detached from the wood cells after combustion at 500 °C (no polymorphic transformation occurred under this experimental condition). A group of polarized optical microscopic (POM) images shows that these individual rod-shaped particles are characteristic of uniform birefringent contrast when being rotated under polarizers, which suggests a high crystallinity and single

crystalline-like nature[37] (Figure 2b). Moreover, both Raman spectrum (Figure 2c) and XRD patterns (Figure s3) unambiguously confirm that these crystals are calcitic $CaCO_3$ with high purity, as the bands at 281 cm^{-1}, 711 cm^{-1}, and 1085 cm^{-1} in the Raman spectrum are assigned to asymmetric stretching of calcite, *in-plane* bending, and symmetric stretching, respectively[38].

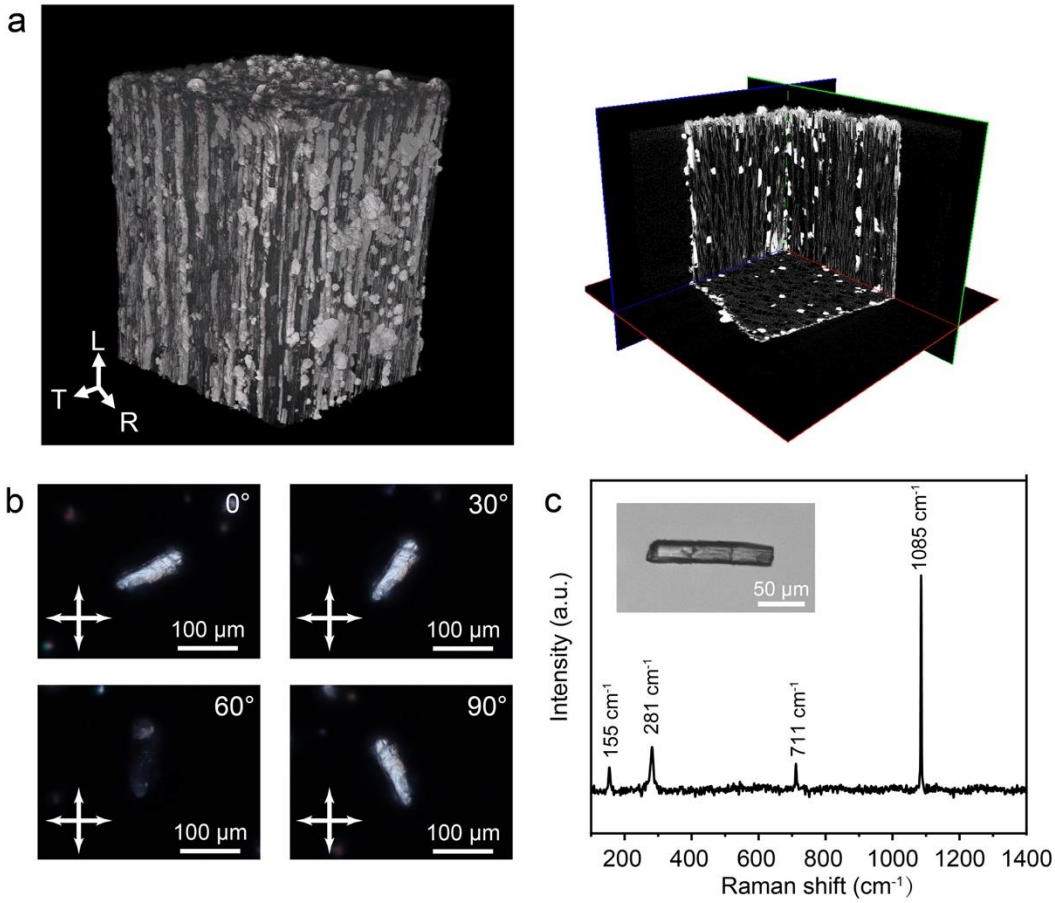
a
L
T
R
b
0°
30°
60°
90°
100 μm
c
50 μm
Intensity (a.u.)
155 cm-1
281 cm-1
711 cm-1
1085 cm-1
200 400 600 800 1000 1200 1400
Raman shift (cm-1)
d
Cell wall
CaCO3
Fiber
25 μm
CaCO3
Cell wall
Fiber
5 μm
Cell wall
CaCO3
500 nm
e
R
L
50 μm
20 μm
1 μm
f
100 nm
g
(110)
5 nm-1
h
d(110)
10 nm

Figure 2. Structural characterization of the $CaCO_3$ mineral embedded in wood cells. (a) Micro computed X-ray tomography images showing the shape of the $CaCO_3$ mineral in the mineralized wood. (b) Rotating POM images of a combustion residue. (c) Raman spectrum of an exemplary $CaCO_3$ microparticle (see the inserted optical microscopic image). (d-e) SEM images showing the structural characteristics of the transverse surface (d) and the radial surface (e) of a mineralized wood. (f-h) Transmission electron microscopic (TEM) image (f), selected area electron diffraction pattern (g), and high-resolution TEM image (h) of a fractured calcite piece. The particles in images c and d were detached from the wood matrices after the combustion treatment.

SEM imaging provides the microstructural information of the mineral particle growth in vessels and axial fibers. The transverse section of the mineralized wood displays that the local space of the vessel was filled with particles (Figure 2d). The $CaCO_3$ growth also occurred in the lumina of wood fibers. The longitudinal section of the wood block exposed the rod-shaped minerals, which were aligned along the elongation direction of the vessel. Different from the classical rhombohedral shape of single crystalline calcite, rod-shaped calcite was evolved ascribed to the specific mineralization microenvironment, as the mineralization proceeded preferentially along the axial direction of the vessel because of the easiness of permeation of reactants to the growth front. The topographic information of the surface of microrods in a vessel is particularly instructive because of the appearance of protruding microdomains that are reminiscent of the pits on the cell wall of the vessels (Figure 2e). It is hypothesized that when the size of a growing microrod is close to that of the vessel diameter, the diffusion of the reactant is not only along the longitudinal direction but through the pits connecting the lumina of the vessels. In principle, the presence of

many protruding microdomains on the embedded $CaCO_3$ microrods can increase the integration between calcitic crystals and cellular walls.

A high magnification SEM imaging on the rapture of a protruding area reveals that the mesoscopic structure of the microrod is composed of densely-packed nanograins (Figure 2e). This piece of information is particularly instructive, as it evidently confirms that the formation of the microrods could undergo a non-classical, nanoparticle-accretion process due to the presence of PAsp[39, 40]. The transmission electron microscopic (TEM) image depicts that the fractured mineral piece is composed of densely-packed nanograins (Figure 2f). Additionally, a selected area electron diffraction (SAED) pattern consists of diffraction spots, which suggests the single crystalline-like structure of the mineral (Figure 2g). Moreover, a high-resolution TEM image discloses that adjacent nanocrystalline domains are crystallographically ordered (Figure 2h). Hence, the TEM finding (Figure 2f-h), together with the uniform birefringent contrast under the polarizers (Figure 2b), confirms the mesocrystalline nature of the microrods[41]. The mesocrystalline nature is evidence for the growth scenario of a microrod starting from a single nucleation site (Figure 3a). Owning to its crystallographic ordering, the mesocrystalline candidate should exhibit a better reinforcement effect compared to its polycrystalline counterparts.

The urease concentration in wood was varied to optimize the protocol of enzymatic mineralization in the current study. The urease concentrations of 5.0 g L^{-1} and 7.0 g L^{-1} gave rise to mineral deposition in wood, as was disclosed in the massive increase of the mineralized wood (Figure 3b). Both experiments demonstrate that the increased concentration of urease in wood cell lumina could cause the relatively high local concentrations of bicarbonate anions and consequently the increased mineral deposition. The establishment of a high supersaturation level within urease–loaded wood is therefore pivotal to the massive deposition of $CaCO_3$ mineral *in-situ*. On the other

hand, a further increase of urease load to a value of 9.0 g L^{-1}, though led to the massive deposition in wood cells, caused the unselective precipitation of $CaCO_3$ mineral. The precipitation occurring in the bulk phase can be ascribed to the high concentration of bicarbonate anions in the surroundings. The precipitates were a mixture of calcite and vaterite, the latter of which belongs to a metastable polymorphic form of $CaCO_3$ mineral and shows moderate mechanical performance when compared with its calcitic counterpart (Figure 3c). Based on the above information, it can be inferred that the concentration of urease anchored in wood determines not only the local concentration of bicarbonate anions but also its concentration gradient in wood and its surroundings.

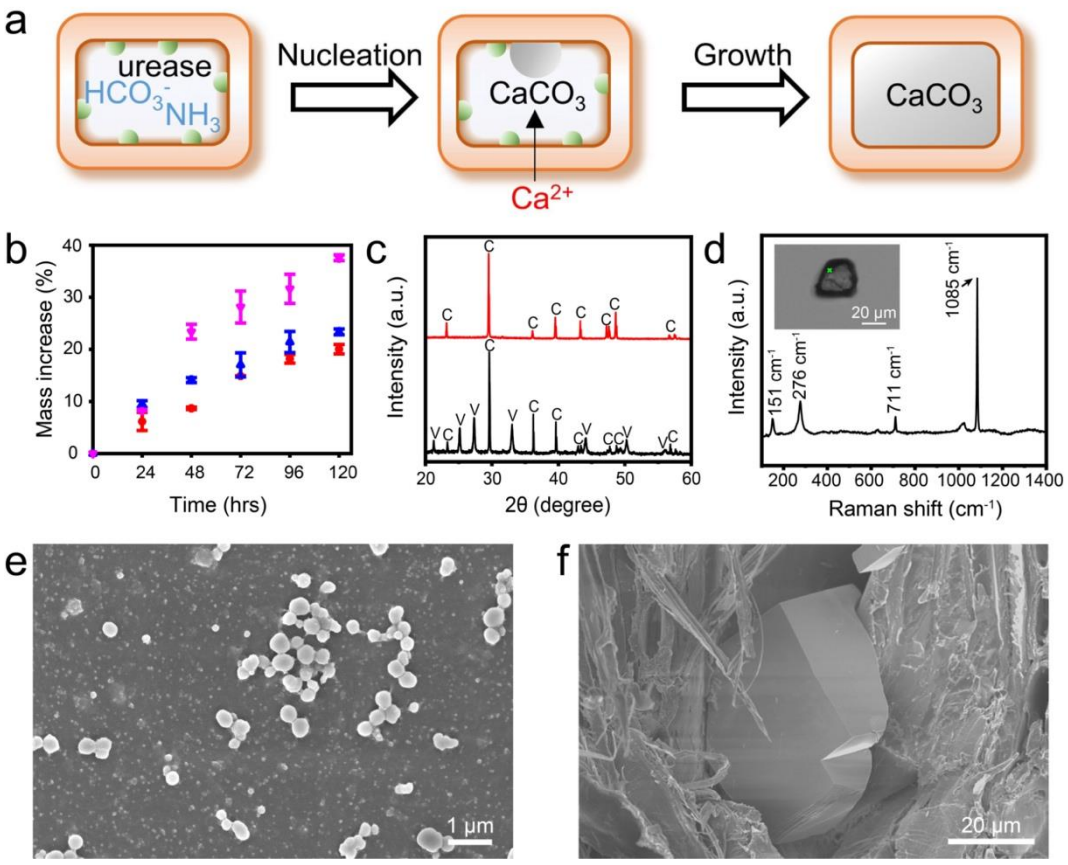

Figure 3. (a) Schematic depiction of the deposition of $CaCO_3$ mesocrystals in urease-immobilized wood. (b) Statistics of the time-resolved mass increases in the mineralized wood, when the urease

concentrations were 5 g L^{-1} (red spheres), 7 g L^{-1} (blue triangles), and 9 g L^{-1} (pink triangles), respectively. (c) XRD patterns of the mineralized products collected from the mineralized wood when the urease concentrations were 7 g L^{-1} (red line) and 9 g L^{-1} (black line), respectively. The abbreviations, namely "C" and "V" in the XRD patterns, denote calcite and vaterite, respectively. (d) Raman spectrum of the mineralized product in wood, which is the combustion residue and depicted in the inserted optical microscopic image. (e-f) SEM images of the radial surfaces showing aggregated nanoparticles on the cell wall of a lumen and rhombohedral-shaped single crystalline calcite. The images e and f were collected using the wood samples enduring mineralization periods of 12 hrs and 48 hrs, respectively). The particles in images c and d were detached from the wood matrices after the combustion treatment.

As mentioned previously, the presence of the PAsp components played an indispensable role in the deposition of $CaCO_3$ mesocrystals in wood cell lumina. The schematic depiction of the deposition of $CaCO_3$ mesocrystals confirms that the mineral deposition in cell lumina endured a multistage process (Figure 3a), namely non-classical mineralization[39, 40]. The presence of 0.01 g L^{-1} PAsp in the reacting liquor witnessed the appearance of aggregated nanoparticles on the surface of cell walls (Figure 3e), which is hypothesized to be amorphous in nature[42]. Subsequently, scattered microcrystals with the sizes of 1-10 μm appeared and were associated with the cell wall, which were probably transformed from the aggregated nanoparticles via the dissolution-recrystallization pathway. Afterwards, these microcrystals evolved into the pseudo-dodecahedral shape, which was ascribed to the presence of the PAsp components in the course of mineralization that controlled the crystal structure by affecting the relative growth rates of different crystal faces[43, 44] (Figure 3f). Raman microscopy was employed to confirm the calcitic form of an exemplary

pseudo-dodecahedral microcrystal in the vessel, where bands at 281 cm^{-1}, 711 cm^{-1}, and 1085 cm^{-1} could be assigned to asymmetric stretching of calcite, *in-plane* bending, and symmetric stretching, respectively[38] (Figure 3d). It is worth noting that the aspect ratios of these microcrystals were roughly unity when their sizes were significantly smaller than those of the vessel diameters. With time, these microcrystals expanded in 3D and started to grow preferentially along the longitudinal direction of wood when their size was comparable with the diameter of the vessels. When the microcrystals completely filled the vessels, the reactants could only be transported to both ends of the mineral in the longitudinal directions, which caused the formation of rod-shaped calcitic mesocrystals in vessels. The growth scenario was therefore in line with the SEM finding (Figure 2a-b). The large aspect ratios of the rod-shaped mesocrystals, together with the occurrence of many protruding microdomains extending into the cell wall pits, favored the interactions between the mineral and wood cells.

Additionally, due to the limitation of the urease activity period, the mineral deposition could last no longer than six days (Figure s2). Therefore, repetitive mineralization was employed to accomplish mineral deposition in wood. The total mass of the mineralized wood increased steadily with the increase of the circulation number (Figure 4a) till the value reached a plateau after two rounds, which implies that the vast majority of wood cells were blocked by minerals and urease could not diffuse into the wood structure for the *in-situ* hydrolysis of urea.

It is imperative that three-circle mineralization proceeding in wood cells started on cell wall surfaces – a heterogeneous crystallization process that ensured the subsequent mineral growth *in-situ* (Figure 3e-f). The selective mineralization on the cell wall surface is ascribed to the synergistic effect of the chemistry of the cell wall and the employment of the PAsp components in the course of mineralization[36]. In the reacting mother liquor, calcium cations and the carboxyl groups on PAsp

can form nanocomplexes[45], which, owing to their high interfacial energy and weakly-charged nature, are adsorbed on cellular walls where waterproof lignin is enriched[11]. Meanwhile, the presence of a low amount of negatively-charged glycoproteins may also facilitate the adsorption of nanocomplex precursors and function as heterogeneous nuclei of multistage mineralization, as well[13]. Therefore, cell walls, in the presence of the PAsp components, enrich calcium cations for *in-situ* deposition of $CaCO_3$ minerals. Similarly, in a study of biomineralization, the appearance of nanogranules on an insoluble organic coccolith scaffold was detected in *in-vitro* mineralization in the presence of coccolith-associated soluble biomacromolecules[36]. These nanocomplexes can be transformed into amorphous and $CaCO_3$ microcrystals in the upcoming stages of multistage mineralization stepwise.

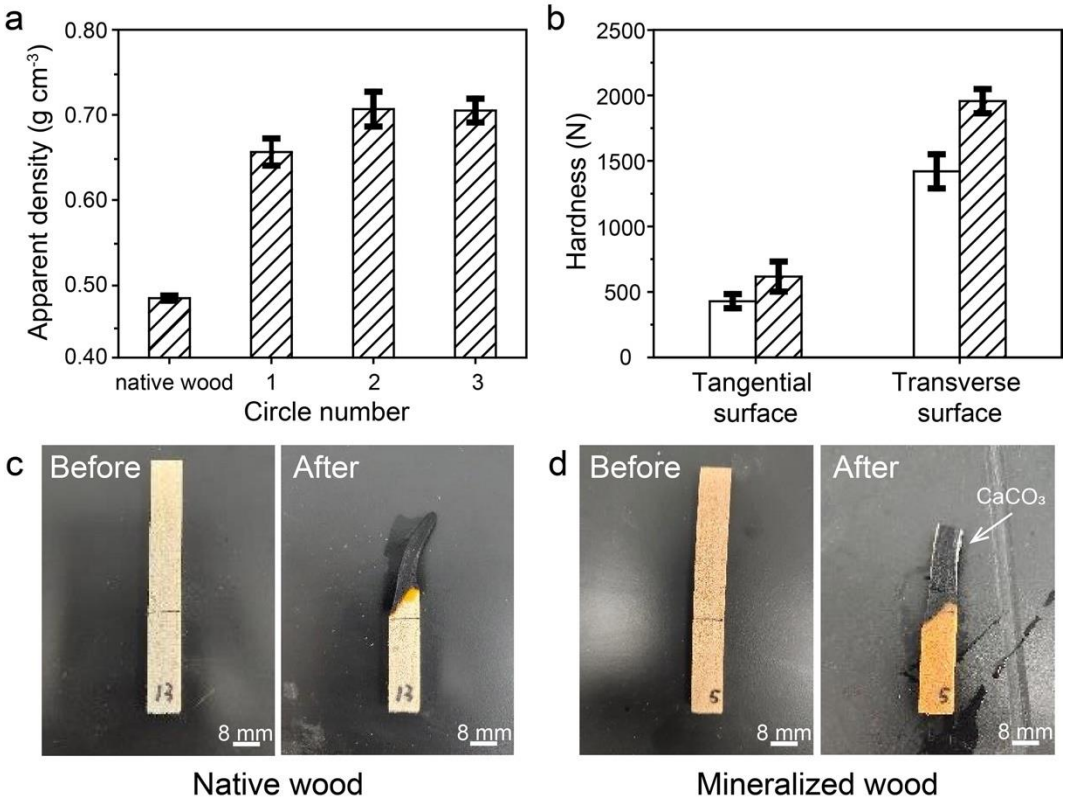

Figure 4. (a) The correlation between the mineralization circle number and apparent density. (b) Surface hardness of the tangential and transverse surfaces of native wood and the mineralized

wood. (c-d) Photographs of native wood (c) and the mineralized wood (d) before and after the limited oxygen index tests, respectively. A continuous layer white in color (see the white arrow in image d) can be observed at the edge of the mineralized wood after the combustion test, which is assumedly ascribed to $CaCO_3$ deposits.

The mechanical performance of the mineralized wood was evaluated by surface hardness tests. The surface hardness of the mineralized wood was evaluated, as mineralization occurred preferentially in cells close to wood surfaces. The hardness values of the tangential surfaces of the mineralized and native woods were 617.0 ± 114.6 N (parallel testing number N = 2) and 429.5 ± 54.4 N (N = 2), respectively (Figure 4b). Similarly, the hardness of the transverse surfaces of the mineralized wood (1956.0 ± 92.3 N, parallel testing number N = 3) was 38% higher than that of native wood (1420.3 ± 130.0 N, N = 3). The increase in the hardness of the mineralized wood was ascribed to the incorporation of the mesocrystalline deposit in cells adjacent to the exterior surface of the wood, which substantially increased the local density of the mineralized wood and compensated for the appearance of the defects of the cellular walls under external force.

The deposition of $CaCO_3$ minerals also caused the improvement of the fire resistance of wood (Figure 4c-d). Limited oxygen index (LOI) was employed to evaluate the flammability of the mineralized wood. The LOI value of the mineralized wood is about 24.4%, and therefore can be classified as the combustible material[24, 46]. As a comparison, the LOI value of native poplar wood is 19.8%, which belongs to the flammable material. The impregnation of mesocrystalline $CaCO_3$, therefore, caused the enhancement of the flame retardancy of the poplar wood, as their spatial distribution close to the surface could inhibit heat transfer, diffusion of oxygen interiorly, and volatilization of flammable gas[36].

CONCLUSIONS

The current paper presents that enzymatic mineralization successfully enriched wood cells with mesocrystalline deposits. The formation of the microrods undergoes a non-classical, nanoparticle-accretion process, starting with the enrichment of calcium cations on the surface of wood cell walls. The subsequent crystal growth was along the longitudinal direction of the wood, resulting in the impregnation of mesocrystalline calcitic microrods in wood cells including vessels and fibers. The coupling of the wood surface with $CaCO_3$ minerals gives rise to mechanical protection and support of the relatively soft wood tissues interiorly. Additionally, the mineralized constituents act as a non-flammable layer for the wood to inhibit heat transfer and volatilization of flammable gas, improving the flame-retardant capacity of the mineralized wood. The method can be extended to other functional minerals with emerging properties, where the mineralization strategy gives rise to the precise control of structural forms, which in turn have a direct impact on the properties of the mineralized wood.

ASSOCIATED CONTENT

Supporting Information

The Supporting Information is available free of charge.

Detailed experimental procedures including Materials, Methods, Characterization, Hardness tests, and Fire-regardant properties; Figures and ATR-FTIR spectra of the urease loaded wood; Change of the pH values showing urease activity in the course of six days; XRD patterns of calcite standard and the combustion residue showing the mineralized products belong to calcite; and a related reference (PDF).

AUTHOR INFORMATION

Corresponding Authors

*Yuan Jiang – College of Materials, State Key Laboratory of Marine Environmental Science, Fujian Key Laboratory of Advanced Materials, Higher Educational Key Laboratory for Biomedical Engineering of Fujian Province, Xiamen University, Xiamen 361005, P.R. China; State Key Laboratory of Silicon Materials, Zhejiang University, Hangzhou 310027, P.R. China; Email: yuan.jiang@xmu.edu.cn

*Lei Ren – College of Materials, State Key Laboratory of Marine Environmental Science, Fujian Key Laboratory of Advanced Materials, Higher Educational Key Laboratory for Biomedical Engineering of Fujian Province, Xiamen University, Xiamen 361005, P.R. China; Email: renlei@xmu.edu.cn

Authors

Tian Fei – College of Materials, State Key Laboratory of Marine Environmental Science, Fujian Key Laboratory of Advanced Materials, Higher Educational Key Laboratory for Biomedical Engineering of Fujian Province, Xiamen University, Xiamen 361005, P.R. China

Han-Jing Yi – College of Materials, State Key Laboratory of Marine Environmental Science, Fujian Key Laboratory of Advanced Materials, Higher Educational Key Laboratory for Biomedical Engineering of Fujian Province, Xiamen University, Xiamen 361005, P.R. China

Robert Zboray – Centre for X-ray Analytics, Empa Dübendorf, 8600 Dübendorf, Switzerland

Xiao-Qiang Yan – College of Materials, State Key Laboratory of Marine Environmental Science, Fujian Key Laboratory of Advanced Materials, Higher Educational Key Laboratory for Biomedical Engineering of Fujian Province, Xiamen University, Xiamen 361005, P.R. China

Si-Si Song – College of Materials, State Key Laboratory of Marine Environmental Science, Fujian Key Laboratory of Advanced Materials, Higher Educational Key Laboratory for Biomedical Engineering of Fujian Province, Xiamen University, Xiamen 361005, P.R. China

Huizhang Guo – Wood Materials Science, ETH Zürich, 8093 Zürich, Switzerland

Author Contributions

The manuscript was written through contributions of all authors. All authors have given approval to the final version of the manuscript.

Notes

The authors declare no competing financial interest.

ACKNOWLEDGMENT

We acknowledge the financial support from the National Natural Science Foundation of China (21875193 & 22075235) and from State Key Laboratory of Silicon Materials (SKL2022-02). We thank Prof. Dr. Helmut Cölfen & Prof. Dr. Ingo Burgert for scientific discussion and constructive comments. We thank Mr. Xiuming Zhang for wood cutting and sampling technology assistance. Prof. Youhui Lin, Drs. Yanan Sun, Likun Yang & Jinming Wang, Zhaohui Meng, Yange Wang,

Kaibin He, and Shengshi Guo are acknowledged for synthesis and characterization assistance. We thank Wei Liu for providing pristine wood samples for experiments.

REFERENCES

1. Gibson, L. J.; Ashby, M. F., *Cellular Solids: Structure and Properties*. 2 ed.; Cambridge University Press: Cambridge, 1997, DOI: 10.1017/CBO9781139878326.

2. Gibson, L. J.; Ashby, M. F.; Harley, B. A., *Cellular Materials in Nature and Medicine*. Cambridge Univ. Press: 2010.

3. Gustavsson, L.; Pingoud, K.; Sathre, R., Carbon Dioxide Balance of Wood Substitution: Comparing Concrete- and Wood-Framed Buildings. *Mitigation Adapt. Strategies Global Change* 2006, *11* (3), 667-691, DOI: 10.1007/s11027-006-7207-1.

4. Burgert, I.; Cabane, E.; Zollfrank, C.; Berglund, L., Bio-inspired functional wood-based materials – hybrids and replicates. *Int. Mater. Rev.* 2015, *60* (8), 431-450, DOI: 10.1179/1743280415Y.0000000009.

5. Ramage, M. H.; Burridge, H.; Busse-Wicher, M.; Fereday, G.; Reynolds, T.; Shah, D. U.; Wu, G.; Yu, L.; Fleming, P.; Densley-Tingley, D.; Allwood, J.; Dupree, P.; Linden, P. F.; Scherman, O., The wood from the trees: The use of timber in construction. *Renewable Sustainable Energy Rev.* 2017, *68*, 333-359, DOI: 10.1016/j.rser.2016.09.107.

6. Wimmers, G., Wood: a construction material for tall buildings. *Nat. Rev. Mater.* 2017, *2* (12), 17051, DOI: 10.1038/natrevmats.2017.51.

7. Song, J.; Chen, C.; Zhu, S.; Zhu, M.; Dai, J.; Ray, U.; Li, Y.; Kuang, Y.; Li, Y.; Quispe, N.; Yao, Y.; Gong, A.; Leiste, U. H.; Bruck, H. A.; Zhu, J. Y.; Vellore, A.; Li, H.; Minus, M. L.; Jia, Z.; Martini, A.; Li, T.; Hu, L., Processing bulk natural wood into a high-performance structural material. *Nature* 2018, *554* (7691), 224-228, DOI: 10.1038/nature25476.

8. Eder, M.; Schäffner, W.; Burgert, I.; Fratzl, P., Wood and the Activity of Dead Tissue. *Adv. Mater.* 2021, *33* (28), 2001412, DOI: 10.1002/adma.202001412.

9. Côté, W. A., The Structure of Wood and the Wood Cell Wall. In *Principles of Wood Science and Technology: I Solid Wood*, Kollmann, F. F. P.; Côté, W. A., Eds. Springer Berlin Heidelberg: Berlin, Heidelberg, 1968; pp 1-54, DOI: 10.1007/978-3-642-87928-9_1.

10. Trtik, P.; Dual, J.; Keunecke, D.; Mannes, D.; Niemz, P.; Stähli, P.; Kaestner, A.; Groso, A.; Stampanoni, M., 3D imaging of microstructure of spruce wood. *J. Struct. Biol.* 2007, *159* (1), 46-55, DOI: 10.1016/j.jsb.2007.02.003.

11. Côté, W. A., Chemical Composition of Wood. In *Principles of Wood Science and Technology: I Solid Wood*, Kollmann, F. F. P.; Côté, W. A., Eds. Springer Berlin Heidelberg: Berlin, Heidelberg, 1968; pp 55-78, DOI: 10.1007/978-3-642-87928-9_2.

12. Sjöström, E., Chapter 1 - THE STRUCTURE OF WOOD. In *Wood Chemistry (Second Edition)*, Sjöström, E., Ed. Academic Press: San Diego, 1993; pp 1-20, DOI: 10.1016/B978-0-08-092589-9.50005-X.

13. Chen, C.; Kuang, Y.; Zhu, S.; Burgert, I.; Keplinger, T.; Gong, A.; Li, T.; Berglund, L.; Eichhorn, S. J.; Hu, L., Structure-property-function relationships of natural and engineered wood. *Nat. Rev. Mater.* 2020, *5* (9), 642-666, DOI: 10.1038/s41578-020-0195-z.

14. Panzarasa, G.; Burgert, I., Designing functional wood materials for novel engineering applications. *Holzforschung* 2022, *76* (2), 211-222, DOI: 10.1515/hf-2021-0125.

15. Youngs, R.; Erickson, J. R., The challenges of utilizing the changing wood resource of the south. In *North Carolina State University Proceedings*, 1984; pp 53-62.

16. Suzuki, S., Using Cedar Plantation Materials for Wood-Based Composites in Japan. In *Using Wood Composites as a Tool for Sustainable Forestry*, 2005; p 9.

17. Fratzl, P., Wood made denser and stronger. *Nature* 2018, *554* (7691), 172-173, DOI: 10.1038/d41586-018-01371-0.

18. Frey, M.; Biffi, G.; Adobes-Vidal, M.; Zirkelbach, M.; Wang, Y.; Tu, K.; Hirt, A. M.; Masania, K.; Burgert, I.; Keplinger, T., Tunable Wood by Reversible Interlocking and Bioinspired Mechanical Gradients. *Adv. Sci.* 2019, *6* (10), 1802190, DOI: 10.1002/advs.201802190.

19. Guo, H.; Özparpucu, M.; Windeisen-Holzhauser, E.; Schlepütz, C. M.; Quadranti, E.; Gaan, S.; Dreimol, C.; Burgert, I., Struvite Mineralized Wood as Sustainable Building Material: Mechanical and Combustion Behavior. *ACS Sustainable Chem. Eng.* 2020, *8* (28), 10402-10412, DOI: 10.1021/acssuchemeng.0c01769.

20. Lowden, L. A.; Hull, T. R., Flammability behaviour of wood and a review of the methods for its reduction. *Fire Sci. Rev.* 2013, *2*, 4, DOI: 10.1186/2193-0414-2-4.

21. Merk, V.; Chanana, M.; Keplinger, T.; Gaan, S.; Burgert, I., Hybrid wood materials with improved fire retardance by bio-inspired mineralisation on the nano- and submicron level. *Green Chem.* 2015, *17* (3), 1423-1428, DOI: 10.1039/C4GC01862A.

22. Merk, V.; Chanana, M.; Gaan, S.; Burgert, I., Mineralization of wood by calcium carbonate insertion for improved flame retardancy. *Holzforschung* 2016, *70* (9), 867-876, DOI: 10.1515/hf-2015-0228.

23. Guo, H.; Luković, M.; Mendoza, M.; Schlepütz, C. M.; Griffa, M.; Xu, B.; Gaan, S.; Herrmann, H.; Burgert, I., Bioinspired Struvite Mineralization for Fire-Resistant Wood. *ACS Appl. Mater. Interfaces* 2019, *11* (5), 5427-5434, DOI: 10.1021/acsami.8b19967.

24. Yang, X.; Zhang, W., Chapter 11 - Flame Retardancy of Wood-Polymeric Composites. In *Polymer-Based Multifunctional Nanocomposites and Their Applications*, Song, K.; Liu, C.; Guo, J. Z., Eds. Elsevier: 2019; pp 285-317, DOI: 10.1016/B978-0-12-815067-2.00011-1.

25. Hill, C. A. S., *Wood Modification: Chemical, Thermal and Other Processes*. John Wiley & Sons: 2007, DOI:10.1002/0470021748.

26. Mahltig, B.; Swaboda, C.; Roessler, A.; Böttcher, H., Functionalising wood by nanosol application. *J. Mater. Chem.* 2008, *18* (27), 3180-3192, DOI: 10.1039/B718903F.

27. Popescu, C.-M.; Pfriem, A., Treatments and modification to improve the reaction to fire of wood and wood based products—An overview. *Fire Mater.* 2020, *44* (1), 100-111, DOI :10.1002/fam.2779.

28. Dreimol, C. H.; Guo, H.; Ritter, M.; Keplinger, T.; Ding, Y.; Günther, R.; Poloni, E.; Burgert, I.; Panzarasa, G., Sustainable wood electronics by iron-catalyzed laser-induced graphitization for large-scale applications. *Nat. Commun.* 2022, *13* (1), 3680, DOI: 10.1038/s41467-022-31283-7.

29. Dong, X.; Gan, W.; Shang, Y.; Tang, J.; Wang, Y.; Cao, Z.; Xie, Y.; Liu, J.; Bai, L.; Li, J.; Rojas, O. J., Low-value wood for sustainable high-performance structural materials. *Nat. Sustain.* 2022, *5* (7), 628-635, DOI: 10.1038/s41893-022-00887-8.

30. Berglund, L. A.; Burgert, I., Bioinspired Wood Nanotechnology for Functional Materials. *Adv. Mater.* 2018, *30* (19), 1704285, DOI: 10.1002/adma.201704285.

31. Gibson, L. J., The hierarchical structure and mechanics of plant materials. *J. R. Soc. Interface* 2012, *9* (76), 2749-2766, DOI: 10.1089/rsif.2012.0341.

32. Nowak, J.; Nowak, D.; Chevallier, P.; Lekki, J.; Van Grieken, R.; Kuczumow, A., Analysis of composite structure and primordial wood remains in petrified wood. *Appl. Spectrosc.* 2007, *61* (8), 889-895, DOI: 10.1366/000370207781540141.

33. Yu, Z.-L.; Yang, N.; Zhou, L.-C.; Ma, Z.-Y.; Zhu, Y.-B.; Lu, Y.-Y.; Qin, B.; Xing, W.-Y.; Ma, T.; Li, S.-C.; Gao, H.-L.; Wu, H.-A.; Yu, S.-H., Bioinspired polymeric woods. *Science Adv.* 2018, *4* (8), eaat7223, DOI: 10.1126/sciadv.aat7223.

34. Hosoda, N.; Sugawara, A.; Kato, T., Template Effect of Crystalline Poly(vinyl alcohol) for Selective Formation of Aragonite and Vaterite $CaCO_3$ Thin Films. *Macromolecules* 2003, *36* (17), 6449-6452, DOI: 10.1021/ma025869b.

35. Kato, T.; Sakamoto, T.; Nishimura, T., Macromolecular Templating for the Formation of Inorganic-Organic Hybrid Structures. *MRS Bull.* 2010, *35* (2), 127-132, DOI: 10.1557/mrs2010.632.

36. Gal, A.; Wirth, R.; Kopka, J.; Fratzl, P.; Faivre, D.; Scheffel, A., Macromolecular recognition directs calcium ions to coccolith mineralization sites. *Science* 2016, *353* (6299), 590-593, DOI: 10.1126/science.aaf7889.

37. Liu, M.-F.; Lu, Z.; Zhang, Z.; Xiao, C.; Li, M.; Huang, Y.-X.; Liu, X. Y.; Jiang, Y., Correlations of crystal shape and lateral orientation in bioinspired $CaCO_3$ mineralization. *CrystEngComm* 2018, *20* (35), 5241-5248, DOI: 10.1039/C8CE00491A.

38. Wehrmeister, U.; Jacob, D. E.; Soldati, A. L.; Loges, N.; Häger, T.; Hofmeister, W., Amorphous, nanocrystalline and crystalline calcium carbonates in biological materials. *J. Raman Spectrosc.* 2011, *42* (5), 926-935, DOI: 10.1002/jrs.2835.

39. De Yoreo, J. J.; Gilbert, P. U. P. A.; Sommerdijk, N. A. J. M.; Penn, R. L.; Whitelam, S.; Joester, D.; Zhang, H.; Rimer, J. D.; Navrotsky, A.; Banfield, J. F.; Wallace, A. F.; Michel, F. M.; Meldrum, F. C.; Cölfen, H.; Dove, P. M., Crystallization by particle attachment in synthetic, biogenic, and geologic environments. *Science* 2015, *349* (6247), aaa6760, DOI: 10.1126/science.aaa6760.

40. Gal, A.; Kahil, K.; Vidavsky, N.; DeVol, R. T.; Gilbert, P. U. P. A.; Fratzl, P.; Weiner, S.; Addadi, L., Particle Accretion Mechanism Underlies Biological Crystal Growth from an Amorphous Precursor Phase. *Adv. Funct. Mater.* 2014, *24* (34), 5420-5426, DOI: 10.1002/adfm.201400676.

41. Sturm, E. V.; Cölfen, H., Mesocrystals: structural and morphogenetic aspects. *Chem. Soc. Rev.* 2016, *45* (21), 5821-5833, DOI: 10.1039/C6CS00208K.

42. Addadi, L.; Raz, S.; Weiner, S., Taking Advantage of Disorder: Amorphous Calcium Carbonate and Its Roles in Biomineralization. *Adv. Mater.* 2003, *15* (12), 959-970, DOI: 10.1002/adma.200300381.

43. Song, R.-Q.; Xu, A.-W.; Antonietti, M.; Cölfen, H., Calcite Crystals with Platonic Shapes and Minimal Surfaces. *Angew. Chem. Int. Ed.* 2009, *48* (2), 395-399, DOI; 10.1002/anie.200803383.

44. Ihli, J.; Bots, P.; Kulak, A.; Benning, L. G.; Meldrum, F. C., Elucidating Mechanisms of Diffusion-Based Calcium Carbonate Synthesis Leads to Controlled Mesocrystal Formation. *Adv. Funct. Mater.* 2013, *23* (15), 1965-1973, DOI: 10.1002/adfm.201201742.

45. Fantinel, F.; Rieger, J.; Molnar, F.; Hübler, P., Complexation of Polyacrylates by Ca^{2+} Ions. Time-Resolved Studies Using Attenuated Total Reflectance Fourier Transform Infrared Dialysis Spectroscopy. *Langmuir* 2004, *20* (7), 2539-2542, DOI: 10.1021/Ia030354e.

46. John, M. J., Chapter 2 - Flammability performance of biocomposites. In *Green Composites for Automotive Applications*, Koronis, G.; Silva, A., Eds. Woodhead Publishing: 2019; pp 43-58, DOI: 10.1016/B978-0-08-102177-4.00002-1.

SYNOPSIS: Bioinspired mineralization armors native wood with mesocrystalline microrods for reinforcement and improvement of flame-retardancy in a sustainable manner.

TOC

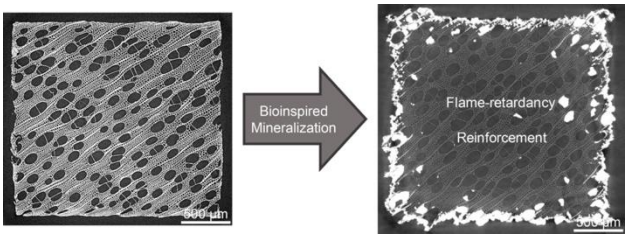

The TOC image is for Table of Contents Use Only.